

# Corrosion Resistance of Diamond-like Carbon-Coated Aluminum Films

C. Srividya and S. V. Babu\*

Center for Advanced Materials Processing and Department of Chemical Engineering,  
Clarkson University, Potsdam, New York 13699

Received February 26, 1996. Revised Manuscript Received June 24, 1996<sup>®</sup>

The corrosion characteristics of diamond-like carbon (DLC) films, deposited on aluminum film-covered single-crystal silicon substrates were investigated using standard potentiometric methods. The DLC films were deposited by radio frequency (13.56 MHz) plasma deposition from three different precursors, methane, acetylene, and 1,3 butadiene, with argon or hydrogen as the diluent. A 5 nm thick polysilicon (PS) film was plasma-deposited prior to DLC film deposition to improve adhesion. The measured corrosion current increased with an increase in the hydrogen content in the feed gas mixture and was lowest for the films deposited from butadiene and highest for those deposited from methane. Also, the DLC films deposited at higher gas flow rates and lower rf powers offered better protection against corrosion than those deposited at lower gas flow rates and higher rf powers. Annealing improved the corrosion resistance. The corrosion currents for certain DLC/PS/Al/Si samples were about 15 times smaller than those for polyimide (PI)/Al/Si samples.

## Introduction

Diamond-like carbon (DLC) films have found use in a variety of applications due to their wide spectrum of highly desirable properties such as hardness, extreme chemical inertness, very high electrical resistivity, smoothness, very low moisture diffusivity, etc. Many of these properties can be varied over a wide range of values by changing the deposition process parameters. DLC films can be deposited using various techniques such as ion beam deposition,<sup>1,2</sup> glow discharge deposition,<sup>3,4</sup> chemical vapor deposition (CVD), plasma-assisted CVD,<sup>5</sup> laser ablation, etc. The DLC films discussed here were deposited in a capacitively coupled 13.56 MHz radio frequency (rf) plasma reactor on unheated substrates.

Hard DLC films are composed of carbon and small amounts, by weight, of hydrogen, the latter in both bonded and unbonded forms. However, in atomic percentages, the hydrogen fraction can be substantial. The structure and properties of these hydrogenated amorphous carbon films depend on the nature of carbon–carbon and carbon–hydrogen bonding as well as the hydrogen content in the film.<sup>5–7</sup> Tamor et al.<sup>8</sup> studied the nature of bonding in hydrogenated amorphous carbon using NMR spectroscopy and quantified four types of bonding configurations for carbon: 4-fold

coordinated and protonated (CH, CH<sub>2</sub>, CH<sub>3</sub>), 4-fold coordinated and unprotonated, 3-fold coordinated and protonated (CH, CH<sub>2</sub>), and, finally, 3-fold coordinated and unprotonated. The relative distribution of these different bonding configurations, which influences film properties such as stress and hardness, was strongly dependent on the negative self-bias voltage. The extent of the different bonding configurations is also influenced by other process variables such as feed gas flow rate, composition, and ion impact energy, which itself is a function of deposition pressure and substrate bias voltage.<sup>5,8,9</sup> The effect of these process variables on the corrosion resistance of DLC films is investigated in this paper to evaluate their suitability for coating Al substrates in general and for encapsulation of intermetallic contacts in multichip modules (MCMs), in particular.

Interconnection between the chips in an MCM is provided by thin-film metal lines which are typically made of aluminum, gold, or copper. Corrosion of metal lines is a major concern in MCMs.<sup>10</sup> Moisture and chloride and alkali ions are some of the contaminants which can corrode the metal wiring. Polyimide/ceramic substrates in which the metal conductors are embedded provide considerable protection to the metallic interconnects.<sup>11</sup> However, polyimide is nonhermetic, has poor thermal conductivity, and is known to interact with copper, degrading the polymer/metal interface.<sup>11,12</sup> DLC films, on the other hand, are known to be chemically inert and have very high thermal conductivity.<sup>13</sup> While Sella et al.<sup>14</sup> demonstrated that DLC films offered

\* Abstract published in *Advance ACS Abstracts*, September 1, 1996.

- (1) Aisenberg, S.; Chabot, R. *J. Appl. Phys.* **1971**, *42*, 2953.
- (2) Spencer, E. G.; Schmidt, P. H.; Joy, D. C.; Sansalone, F. J. *Appl. Phys. Lett.* **1976**, *29*, 118.
- (3) Holland, L.; Ojha, S. M. *Thin Solid Films* **1976**, *L17*.
- (4) Catherine, Y. In *Properties and Characterization of Amorphous Carbon Films*; Pouch, J. J., Alterovitz, S. A., Eds.; Trans Tech Publications: Lebanon, NH, 1989; pp 175–196.
- (5) Angus, J. C.; Koidl, P.; Domitz, S. In *Plasma Deposited Thin Films*; Mort, J., Jensen, F., Eds.; CRC Press: Boca Raton, FL, 1986; p 91.
- (6) Tsai, H.; Bogy, B. B. *J. Vac. Sci. Technol. A* **1987**, *5*, 3286.
- (7) Seth, J.; Babu, S. V. *J. Appl. Phys.* **1993**, *73*, 2496–2504.
- (8) Tamor, M. A.; Vassell, W. C.; Carduner, K. R. *Appl. Phys. Lett.* **1991**, *58*, 592–594.

- (9) Bubenzer, A.; Dischler, B.; Brandt, G.; Koidl, P. *J. Appl. Phys.* **1984**, *54*, 4590.
- (10) Cech, J. M.; Burnett, A. F.; Chien, C.-P. *IEEE Trans. Comp., Hybrids, Manuf. Technol.* **1993**, *16*, 752–758.
- (11) Garrou, P. *Proc. IEEE* **1992**, *80*(12), 1942–1954.
- (12) Adema, G. M.; Hwang, L.-T.; Rinne, G. A.; Turlik, I. *IEEE Trans. Comp., Hybrids, Manuf. Technol.* **1993**, *16*, 53–59.
- (13) Yoshida, M.; Ogawa, K.; Tsuji, H.; Ishikawa, J.; Takagi, T. *Proc. 11th Symp. on ISIT87*; Tokyo, 1987.
- (14) Sella, C.; Lecoeur, J.; Sampeur, Y.; Catania, P. *Surf. Coatings Technol.* **1993**, *60*, 577–583.

excellent corrosion resistance to Ti and Mg, Koskinen et al.<sup>15</sup> reported that DLC coatings are too porous to be used in corrosive environments. However, these films were deposited by the arc discharge method and since film porosity is process-dependent, it might be possible to deposit much less porous and more corrosion-resistant DLC films using other deposition techniques. In this paper, it is shown that, indeed, rf plasma-deposited DLC films offer excellent corrosion protection. The corrosion resistance of DLC films, on Al-film-covered silicon substrates, has been characterized by standard potentiometric methods<sup>16,17</sup> using an electrolyte containing 0.1 M NaCl and 0.1 M Na<sub>2</sub>SO<sub>4</sub> in deionized water. The corrosion protection offered by the DLC films is superior to that provided by polyimide films.

Passive films on metal surfaces act as a physical barrier between the metal surface and the corrosive environment. Such films are rarely devoid of mechanical defects such as cracks, pinholes, etc. Pinholes and cracks allow the corrosive environment to access the metal surface. Anodic reaction occurs at the metal surface which, in the present case, is aluminum dissolution in the NaCl/Na<sub>2</sub>SO<sub>4</sub> electrolyte. The presence of chloride ions accelerates the corrosion rate of aluminum,<sup>18,19</sup> resulting eventually in the dissolution of aluminum around the pinhole or the crack in the film, lifting it off from the substrate. The corrosion current resulting from aluminum dissolution has been used as an indicator of corrosion resistance of the passive films.

Here, the corrosion characteristics of DLC films, deposited in rf plasma discharge using CH<sub>4</sub>, C<sub>2</sub>H<sub>2</sub>, and C<sub>4</sub>H<sub>6</sub> as carbon source gases and argon and hydrogen as diluents, are compared for different process conditions—feed gas flow rate and composition, and rf power. These hydrocarbon gases and the diluents provide a large variation in the overall C/H ratio in the gas phase precursor species. The effect of postdeposition annealing on film corrosion resistance is also studied. The results are compared with those for spin-coated polyimide films on Al-covered silicon substrates.

## Experiment

The experiments consisted of (i) deposition of Al on single-crystal silicon substrates by thermal evaporation, (ii) deposition of DLC films or spin coating of PI films on Al/Si substrates, and (iii) measurement of corrosion current for each of the composite films by potentiostatic methods. A 5 nm thick layer of polysilicon (PS), rf plasma-deposited from a mixture of silane and argon, was used between the Al and DLC films to improve adhesion, resulting in DLC/PS/Al/Si substrates. It is shown later that while the thin PS layer offers enhanced protection to the underlying Al film (Figure 1), the addition of the DLC film reduces the corrosion current density by a further 3 orders of magnitude.

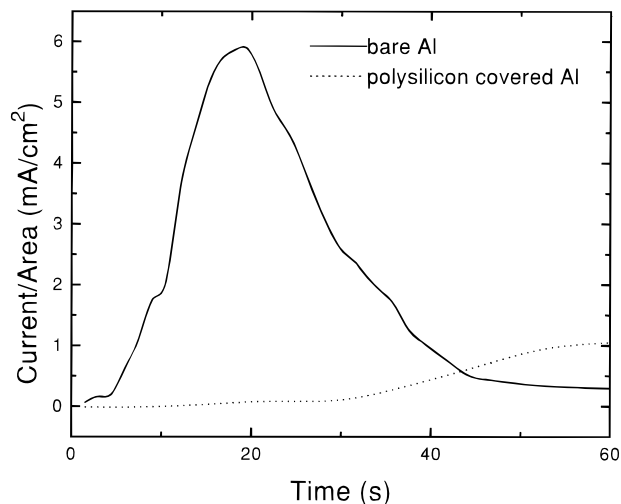


**Figure 1.** Solid line represents the corrosion current density recorded with bare aluminum film; the dotted line showing the corrosion current for polysilicon (PS) is continued for longer times in Figure 6.

The 0.1  $\mu\text{m}$  thick aluminum films were deposited on single-crystal silicon substrates by thermal evaporation from aluminum pellets in a vacuum chamber which was pumped down to a pressure of  $10^{-5}$  Torr using a turbomolecular pump. DLC films were deposited on the aluminum film-covered silicon substrates in a conventional parallel-plate plasma reactor (PlasmaTherm Model 730) described elsewhere.<sup>20</sup> The substrate was placed on the lower powered electrode, maintained nominally at room temperature by circulating a coolant mixture. The process gases—CH<sub>4</sub>, C<sub>2</sub>H<sub>2</sub>, or C<sub>4</sub>H<sub>6</sub> along with Ar or H<sub>2</sub> acting as the diluent—enter the chamber through a shower head in the upper grounded electrode. The unreacted gases were removed by a Roots blower-mechanical pump combination through exhaust ports located at the four corners in the lower wall of the reaction chamber. The base pressure in the chamber was about 1 mTorr. Rf power at 13.56 MHz was delivered to the chamber through an automatic matching network. Reflected power was always less than 2 W. The deposition conditions and the feed gas mixtures used in the preparation of the DLC film samples investigated here are given in Table 1.

Polyimide (DuPont PI 2613 LX) films (PI) were deposited by spin coating on aluminum covered single-crystal silicon substrates. The spin speed was ramped up to 3000 rpm at an acceleration of 60 000 rev/min<sup>2</sup>. The duration of spin was 40 s. The film thickness was typically around 300 nm. After spin coating, the polyimide films were cured by soft-baking at 90 °C for 2 min, at 130 °C for 20 min, followed by a hard-bake at 350 °C for 1.5 h.

**Potentiometry.** The corrosion resistance offered by DLC to the underlying aluminum films was characterized by potentiostatic measurements. A standard calomel electrode (SCE) and a platinum electrode were used as reference and counter electrodes, respectively. The electrolytic solution consisted of 0.1 M NaCl and 0.1 M Na<sub>2</sub>SO<sub>4</sub> in deionized water.

The dimensions of the test samples were typically 25 mm  $\times$  25 mm. The sample edges were covered with

(15) Koskinen, J.; Ehrnstén, U.; Mahiout, A.; Lahtinen, R.; Hirvonen, J.-P.; Hannula, S.-P. *Surf. Coatings Technol.* **1993**, *62*, 356–360.

(16) Fontana, M. G.; Greene, N. D. In *Corrosion Engineering*, 2nd ed.; McGraw-Hill: 1978.

(17) Jones, D. A. In *Principles and Prevention of Corrosion*, 2nd ed.; Prentice Hall: Englewood Cliffs, NJ, 1996.

(18) Kaesche, H. In *Passivity of Metals*; Frankenthal, R. P., Kruger, J., Eds.; The Electrochemical Society: Princeton, NJ, 1978; p 935.

(19) Kaesche, H. In *Localized Corrosion*; Staehle, R. W., et al., Eds.; NACE: Houston, 1974; p 516.

(20) David, M.; Rasmussen, D. H.; Babu, S. V. *AIChE J.* **1990**, *36*, 871.

**Table 1. Process Conditions for DLC Film Deposition (the Deposition Pressure was 25 mTorr for All the Samples)**

sample no.	precursor gas	diluent	feed gas composition (precursor/diluent)	total flow rate (sccm)	rf power (W)	negative bias voltage (V)
1	1,3-butadiene	argon	1/4	120	150	285
2	acetylene	argon	1/4	120	150	285
3	methane	argon	1/4	120	150	275
4	1,3-butadiene	hydrogen	1/4	120	150	295
5	1,3-butadiene	hydrogen	1/9	120	150	290
6	1,3-butadiene	argon	1/4	120	100	230
7	1,3-butadiene	argon	1/4	50	150	280
8	1,3-butadiene	argon	1/4	50	100	240

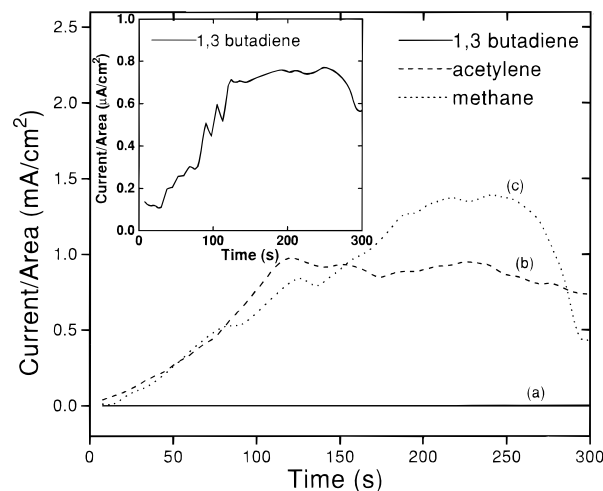
Kapton tape to protect them from the attack of the surrounding electrolytic solution. A three-compartment glass cell was used to hold the sample and the electrodes. It was filled with the electrolytic solution and the test sample was placed in the central compartment. The reference electrode and the counter electrode were placed in the other two compartments separated from the central one by coarse sintered glass. The sample served as the working electrode. An EG&G Princeton Applied Research Model 273A potentiostat–galvanostat was used to apply the controlled potential using an EG&G Princeton Applied Model 352 SoftCorr TM II corrosion software.

Initially, dynamic measurements were made by sweeping the potential applied to a bare Al sample at the rate of 5 mV/s in the range  $-1.5$  to  $+1.5$  V (SCE) and measuring the resulting corrosion current as a function of the applied potential. The pitting potential, i.e., the potential above which corrosion of the anode (the test sample), occurs in the electrolytic solution, was found to be  $-0.8$  V with respect to the SCE. Hence, a controlled voltage of 0.0 V (SCE) was applied to all the sample structures during the subsequent potentiostatic measurements. While this was well below the potential at which the solvent breakdown occurs, it still ensured a zero induction time for the corrosion of the test sample.

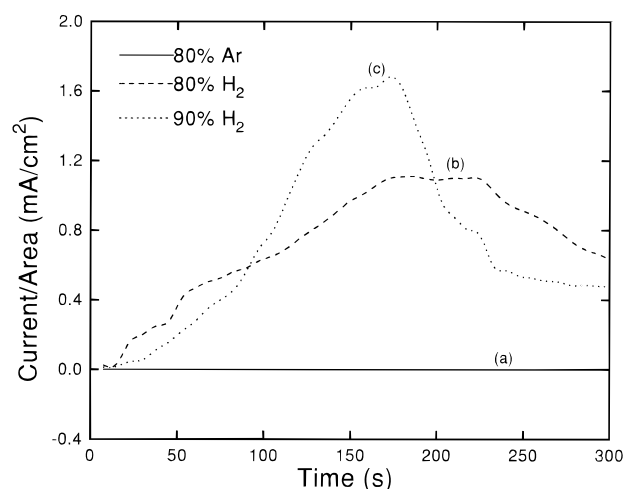
## Results and Discussion

Figure 1 shows the corrosion current densities registered by bare aluminum and polysilicon-covered aluminum films on single-crystal silicon substrates. The bare aluminum film starts dissolving right away. The current reaches its peak value in about 20 s and then starts falling till it reaches zero around 45 s. At this point the Al film had almost completely dissolved in the electrolytic solution. Both the peak current ( $6 \text{ mA/cm}^2$ ) and the time it takes to reach this value (20 s) are representative of the rate and the extent of corrosion occurring in the film. Corrosion current values are also given in Figure 1 for polysilicon (PS)-covered aluminum film. These values for the bare and PS-covered Al films serve as a reference for evaluating and comparing the potential of DLC and PI films in protecting the underlying aluminum film from corrosion. The corrosion current for PS/Al/Si sample shown in Figure 1 is lower than that for the bare aluminum film. However, as discussed later, it still is about 3 orders of magnitude higher than those for DLC/PS/Al/Si samples described below (see Figure 6).

**Precursor Gas Effects.** Figure 2 compares the corrosion current densities measured with the DLC/PS/Al/Si samples, prepared using three different carbon source gases—1,3-butadiene, acetylene, and methane.



**Figure 2.** Curves (a), (b), and (c) represent the corrosion current densities measured with samples 1, 2, and 3 (see Table 1), respectively. Curve (a) is also shown in the inset which gives the corrosion current density in  $\mu\text{A/cm}^2$ .



**Figure 3.** Curves (a), (b), and (c) represent the corrosion current densities measured with samples 1, 4, and 5 (see Table 1), respectively.

Argon (80%) was used as the diluent in all three cases. The films deposited from butadiene offered the best protection while those deposited from methane offered the least protection against corrosion, with the films prepared using acetylene in the middle.

Figure 3 shows the corrosion current densities recorded with DLC/PS/Al/Si structures, prepared from  $\text{C}_4\text{H}_6/\text{Ar}$  and  $\text{C}_4\text{H}_6/\text{H}_2$  feed gas mixtures. The current density increases with an increase in the hydrogen content in the feed gas mixture. This is consistent with the corrosion behavior observed above with the DLC films deposited from the three different precursor gases. The corrosion currents for two samples annealed in

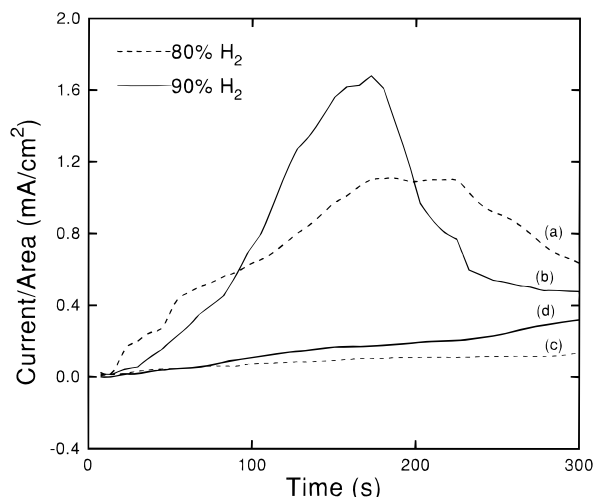


**Figure 4.** Curves (a) and (b) represent the corrosion current densities measured with samples 4 and 5 (see Table 1), respectively; curves (c) and (d) represent those measured with the same samples after annealing.

argon at 250 °C for an hour are shown in Figure 4. Annealing improves the corrosion resistance of the DLC films substantially.

In the present case, two kinds of film failure were observed when potentiostatic measurements were carried out on DLC-coated aluminum films. In the case of films which registered corrosion current densities of the order of  $\mu\text{A}/\text{cm}^2$ , the films (both DLC and Al) were lifted off at random from the silicon substrate at one or two spots. The rest of the film was intact, suggesting that whatever be the defects or flaws that caused the film failure, they were not distributed over the entire film but confined to one or two specific locations in the film. In the case of DLC films which registered corrosion current densities of the order of  $\text{mA}/\text{cm}^2$ , the films were almost completely lifted off during the measurement. Presumably, there is a higher concentration of defects distributed over the entire film. It is also possible that a few defects combined with the residual stress in the films (DLC films are always deposited with a large compressive stress in the film) could have brought about the disbondment of the films. There are several reports published suggesting that internal stress in films of metals and alloys enhances corrosion.<sup>21</sup> Ulrich et al.<sup>22,23</sup> conducted potentiostatic measurements on silicon nitride-covered aluminum films and found that beyond a certain thickness of the nitride film, the corrosion current increased, instead of decreasing, with increasing film thickness. They attributed this behavior to a change in the ultimate strain and the intrinsic stress in the nitride film with changing film thickness. Koskinen et al.<sup>15</sup> arrived at a similar conclusion when thinner DLC films offered more resistance to corrosion than thicker films.

Koskinen et al.<sup>15</sup> have demonstrated that film porosity, as measured by electrochemical impedance spectroscopy (EIS), should be "low" if the films are to provide adequate protection against corrosion. They observed that filtering out particles from the plasma reduced film

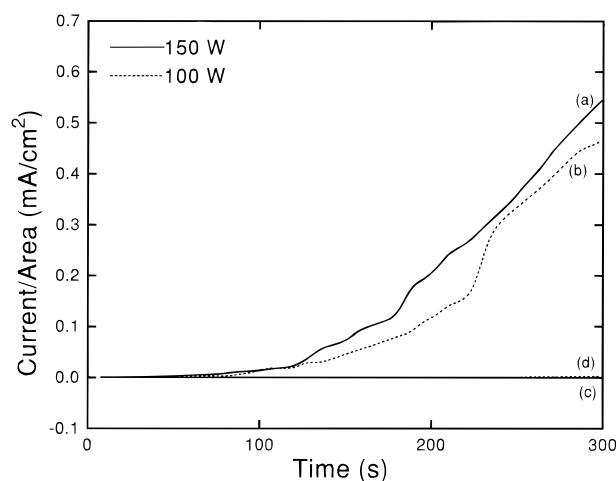


**Figure 5.** Curves (a), (b), (c), and (d) represent the corrosion current densities measured with samples 7, 8, 1, and 6 (see Table 1), respectively. Higher gas flow rate (120 vs 50 sccm) reduces the corrosion current significantly.

porosity and enhanced corrosion resistance. On the other hand, increasing the percentage of hydrogen in the feed gas mixture increased the hydrogen content and reduced the film density.<sup>14</sup> Argon addition to the feed gas mixture, however, results in denser films,<sup>24</sup> also confirmed in our case by the density values of 2.6 and 0.95  $\text{g}/\text{cm}^3$  measured for the films deposited from argon/butadiene (4/1) and hydrogen/butadiene (9/1) mixtures, respectively. EIS measurements on these films<sup>25</sup> suggest that films deposited from argon/butadiene (4/1) mixtures were not porous, while those deposited from hydrogen/butadiene (9/1) mixtures were porous enough to allow the electrolyte to reach the metal surface resulting in aluminum dissolution.

Koidl et al.<sup>26</sup> observed that optical bandgap, hydrogen content, and  $\text{sp}^3/\text{sp}^2$  ratio of a-C:H films, deposited from different process gases but at a common bias voltage of 400 V, were independent of the precursor gas. They attributed it to the almost complete fragmentation of the precursor gas molecules at high bias voltages. However, at lower bias voltages ( $<400$  V), the choice of the precursor gas influenced the film properties considerably. In the present work, all the films were deposited at 150/100 W rf power and the corresponding negative bias voltages, given in Table 1, were in the range 290–240 V.

**Effect of Rf Power and Gas Flow Rate.** Figure 5 shows the corrosion current densities registered with the DLC films deposited at two different rf powers, 150 and 100 W, respectively, from butadiene/argon mixtures. There is only a slight decrease in the corrosion current density as the rf power is lowered from 150 to 100 W, with the associated negative bias voltage changing by only 50 V (see Table 1). However, films deposited at 300 W failed before they could be tested for corrosion, suggesting excessive internal stresses. In contrast, difficulty in handling the very soft films that resulted at lower rf powers ( $<100$  W) prevented their investigation.

(24) Grill, A.; Patel, V. *Diamond Related Mater.* **1994**, *4*, 62–68.

(25) Srividya, C.; Babu, S. V.; Sunkara, M., manuscript in preparation.

(26) Koidl, P.; Wild, Ch.; Dischler, B.; Wagner, J.; Ramsteiner, M. In *Properties and Characterization of Amorphous Carbon Films*; Pouch, J. J., Alterovitz, S. A., Eds.; Trans Tech Publications: Lebanon, NH, 1989; pp 41–70.

(21) Dull, D. L.; Raymond, L. *Corrosion* **1973**, *29*, 205–212.

(22) Ulrich, R. K.; Yi, D.; Brown, W. D.; Ang, S. S. *Thin Solid Films* **1992**, *209*, 73–79.

(23) Ulrich, R. K.; Yi, D.; Brown, W. D.; Ang, S. S. *Corrosion Sci.* **1992**, *33*, 403–412.

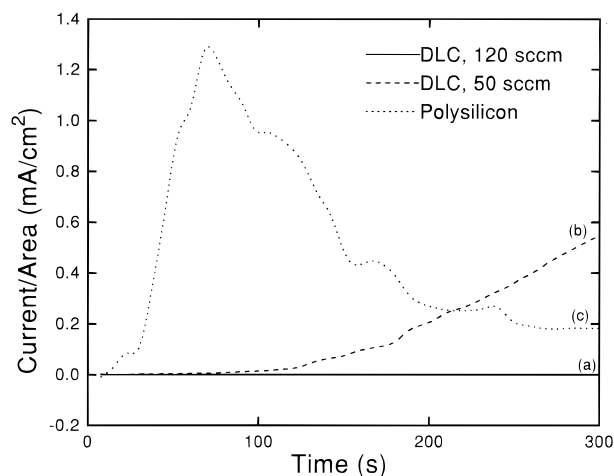


**Figure 6.** Curves (a) and (b) represent the corrosion current densities measured with samples 1 and 7 (see Table 1), respectively; curve (c) represents the corrosion current density for polysilicon (PS) and is also shown in Figure 1 for the first 60 s.

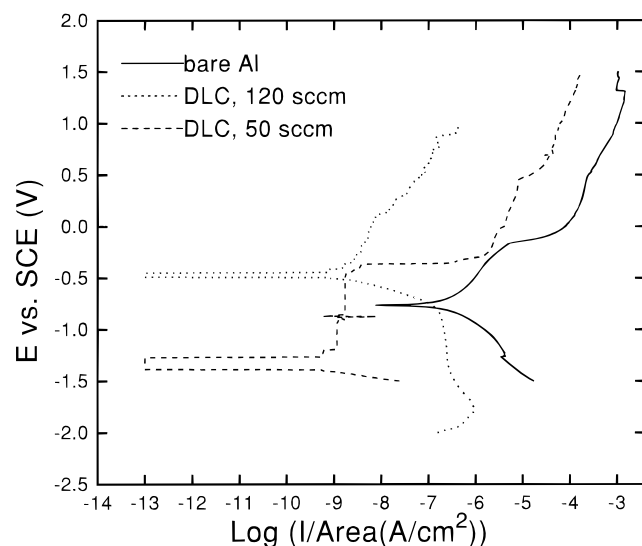


**Figure 7.** Curve (a) represents the polarization curve for bare aluminum while curves (b) and (c) represent the polarization curves for samples 1 and 7 (see Table 1), respectively.

The effect of gas flow rate during DLC film deposition on the current density is shown in Figure 6. The films deposited at a flow rate of 120 sccm are significantly more corrosion resistant than those deposited at a flow rate of 50 sccm. Since the films deposited at 50 sccm were as dense, within experimental error, as those deposited at 120 sccm, the observed difference in the corrosion current density is not due to differences in film density. It is possible that the gas flow rate has a strong influence on the residual stresses in the film, since the films deposited at lower gas flow rates and longer deposition times failed while those deposited at higher gas flow rates remained intact.

These results are confirmed by the polarization curves, shown in Figure 7, for bare aluminum and DLC-covered aluminum films (deposited at 120 and 50 sccm gas flow rates), in an electrolyte consisting of 0.1 M NaCl and 0.1 M Na<sub>2</sub>SO<sub>4</sub> in deionized water. The potential was swept at the rate of 5 mV/s from -2.0 to 1.5 V (SCE). The approximate corrosion current densities  $i_{\text{corr}}$  are listed in Table 2. For the film deposited at 50 sccm,  $i_{\text{corr}}$  is smaller than that for bare Al by a factor

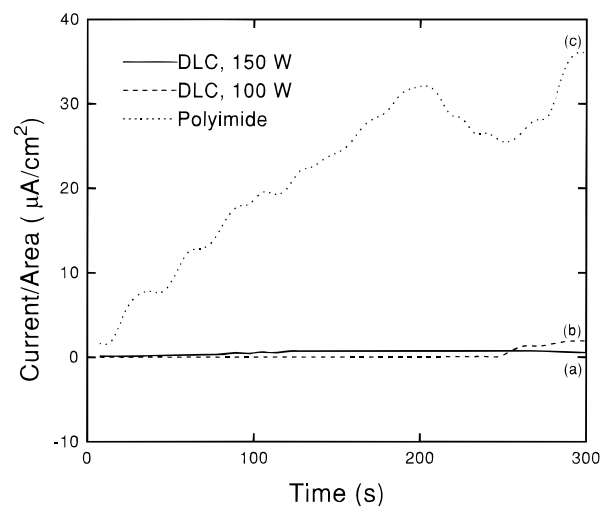


**Figure 8.** Curves (a) and (b) represents the corrosion current densities measured with samples 1 and 6 (see Table 1), respectively; curve (c) represents the corrosion current recorded with polyimide PI 2613 LX film.

**Table 2.**  $E_{\text{corr}}$  and  $I_{\text{corr}}$  Values for Bare Al and Samples 1 and 7

	$I_{\text{corr}}$ ( $\mu\text{A}/\text{cm}^2$ )	$E_{\text{corr}}$ (V)
bare Al	0.91	-0.76
sample 1	0.002	-0.48
sample 7	0.023	-0.88

of 45 and is independent of the potential in the range -1.2 to -0.5 V, which indicates that the corrosion is controlled by the rate of transport of the electrolyte to the underlying metal surface. However, there is a very sharp increase in current beyond -0.5 V, implying aluminum dissolution. Consequently, beyond -0.5 V, this film does not offer good protection against corrosion, a result that is consistent with the higher corrosion current density obtained for this film during the potentiostatic measurements made at 0.0 V. However, below -0.5 V, the film can still provide considerable protection against corrosion. In contrast, for the film deposited at 120 sccm,  $i_{\text{corr}}$  is smaller than that for bare Al by a factor of 450 and is indicative of excellent corrosion protection.

**Comparison of DLC and PI Films.** Figure 8 compares the corrosion currents measured with DLC/PS/Al/Si samples, prepared under two different DLC film deposition conditions, with that from a polyimide PI2613 (PI)/Al/Si sample. Comparing Figures 8 and 1, it can be seen that the corrosion current densities registered with both DLC and PI films are substantially smaller than those recorded with bare aluminum films. However, and more importantly, the corrosion current for the DLC/PS films, deposited at 120 sccm gas flow rate and 150/100 W rf power, is more than 15 times lower than that for the PI film. Thus, these DLC films offer corrosion protection that is far superior to that offered by polyimide PI2613.<sup>27</sup>

**Role of Polysilicon Adhesion Promotion Layer.** Figures 1 and 6 suggest that while PS improves the corrosion resistance of the underlying Al layer, it is certainly not responsible for the dramatic improvements shown in Figures 2–8. Indeed, the 5 nm thick poly-

(27) Babu, S. V.; Srividya, C. U.S. Patent Application, filed May 1996.

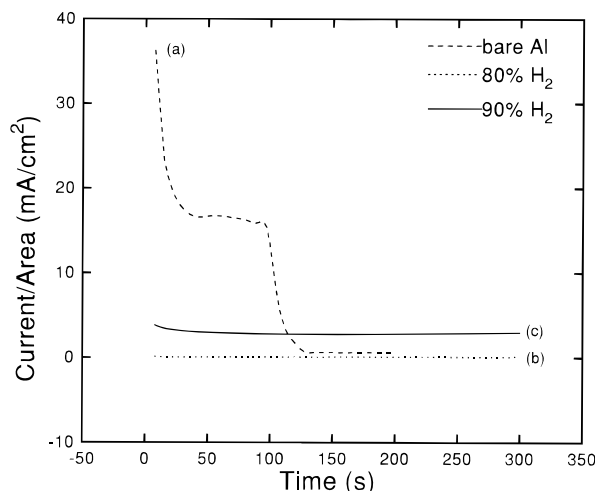


**Figure 9.** Curve (a) represents the corrosion current density measured with bare aluminum film, while curves (b) and (c) represent the corrosion currents for samples 4 and 5 (see Table 1), respectively.

silicon layer reduces the corrosion current by at most a factor of 5 and stretches out the dissolution time to about 80 s. However, when compared with the corrosion currents ( $\sim 1 \mu\text{A}/\text{cm}^2$ ) and the dissolution times ( $> 300$  s) observed for DLC-coated aluminum films, these values are significantly inferior. While experiments with thicker PS films (up to 180 nm thick) show that corrosion current densities are considerably lower, they are still almost 2 orders of magnitude larger than those recorded with DLC-coated samples. Thus the unambiguous conclusion is that the dramatic improvement ( $\sim 3$  orders of magnitude reduction in the corrosion current density in the best case) is attributable to the DLC film only.

**Corrosion Measurements in NaOH Solution.** Figure 9 shows the corrosion current densities for bare Al and DLC/PS/Al sample structures in 0.1 M NaOH

in deionized water for two DLC films prepared from two different concentrations of  $\text{C}_4\text{H}_6/\text{H}_2$  mixtures. Both the DLC films reduced the corrosion current density significantly. Also, as observed with NaCl/ $\text{Na}_2\text{SO}_4$  solutions, DLC films deposited with a higher hydrogen content in the feed gas mixture resulted in larger corrosion current values.

### Summary

Potentiostatic measurements were made on Al/Si, DLC/Al/Si, and PI/Al/Si samples by applying a controlled potential of 0.0 V (SCE) to the samples and recording the resulting corrosion current as a function of time. The electrolyte used was a solution of 0.1 M NaCl and 0.1 M  $\text{Na}_2\text{SO}_4$  in deionized water. In the best case, DLC films reduced the corrosion rate of Al by almost 3 orders of magnitude.

Films deposited from butadiene offered the best protection, while those deposited from methane offered the least protection against corrosion. Films deposited at a higher gas flow rate of 120 sccm were much more corrosion resistant than those deposited at 50 sccm. Annealing improves greatly the protection offered by the films against corrosion.

Finally, the DLC films deposited using butadiene/argon (1:4) feed gas mixture at 120 sccm gas flow rate and 100/150 W rf power generated corrosion currents that are more than 15 times smaller than those for PI (PI2613) films. This observation, combined with the better mechanical properties of DLC films, suggests that DLC films offer a better choice than PI films for encapsulation.

**Acknowledgment.** This work has been supported by grants from Teledyne Electronic Technologies and New York Science and Technology Foundation.

CM9601594